'94 KACC (1994. 10. 17 ~ 20)

On the 3-Dimensional Low Speed Yo-Yo Maneuver

Hiroyuki Takano,* Masaya Sato,** Yoriaki Baba†
Dept. of Aerospace Engineering
National Defense Academy, Japan

Abstract

This paper presents numerical analyses of the low speed yo-yo maneuver of an aircraft to determine controls of thrust, bank-angle and angle-of-attack in the subsonic region in terms of the optimal control theory.

Minimum-time flight paths are numerically calculated to overtake an opponent aircraft flying in some steady-state level turnings under several assumptions: both of aircraft are point masses and maneuver in the 3-Dimensional space. Their weights are considered constant in the maneuver.

As a result of the analyses, the effectiveness of the low speed yo-yo maneuver is shown.

Nomenclature

a : speed of sound
A_W : wing area of aircraft
C_D : drag coefficient
C_{D0} : zero lift drag coefficient
C_L : lift coefficient
$C_{L\alpha}$: lift coefficient curve slope
C_T : thrust coefficient
D : drag
g : acceleration of gravity
I, J : performance index
L : lift
m : aircraft mass
M : Mach number
n : load factor (normal acceleration in g's)
t : time
T : thrust
V : velocity
W : weight of aircraft
x : horizontal position (range)
y : horizontal position (cross range)
z : altitude
α : angle of attack
γ : flight path angle
κ : induced drag factor
ρ : atmospheric density
σ : bank angle
ψ : heading angle

Subscripts

$(\ )_f$: final value
$(\ )_i$: initial value
$(\ )_{max}$: maximum value
$(\ )_{min}$: minimum value
$(\ )_0$: quantity for pursuer
$(\ )_T$: quantity for evader

I. Introduction

Maneuverability is an important factor for many kinds of fighter aircraft to evaluate their performance. Especially, the ability of acceleration, which is one of the indices to define the easiness and smoothness of achieving required maneuver or reaching a position in a definite period of time, often determines the performance superiority of aircraft.

The purpose of this paper is to present flight paths and a set of controls of aircraft for minimum-time 3-Dimensional turn to overtake an opponent aircraft flying in steady-state level turning with some constant velocity and initial distance from the pursuer, in order to verify the system trade-off among the performance components during the optimal maneuver in the 3-Dimensional space. Resulting optimal maneuver for pursuing aircraft turn out to be a low speed yo-yo maneuver, which dive in the first half of the flight to increase the velocity and then rise up in the latter half.

This maneuver can be formulated and resolved with the optimal control theory, which examines in the Sec. II as a general formulation of optimal control problems.

The applications to the formulation of the minimum time-to-overtake problems then are considered in Sec. III, where it is shown that the useful method for formulation with dummy control variable is applied to these problems. In Sec. IV, numerical results of the minimum time-to-overtake problems are presented to illustrate some of the features of optimal trajectories in the situation that an aircraft pursues after an opponent aircraft in front. Some conclusions then are presented in Sec. V

* Lecturer, NDA, Yokosuka, JAPAN, 239
Member SICE
** Graduate student, NDA, Yokosuka, JAPAN, 239
† Professor, NDA, Yokosuka, JAPAN, 239
Member SICE

II. A General Formulation of Optimal Control Problems

Statement of the problem

Consider the system of an aircraft maneuverable in the 3-Dimensional space with the equations of motion

$$\dot{x} = \Phi(x, u, \pi, \tau) \quad (1)$$

The basic problem can be stated as follows. Minimize the functional

$$I = \left[h(z(t_0), \pi, t_0)\right] + \left[g(x(t_f), \pi, t_f)\right] + \int_0^1 f(x, u, \pi, \tau)\, dt \quad (2)$$

with respect to the state $x(\tau)$, the control $u(\tau)$, and the parameter π which satisfy the differential constraints, i.e. the equations of motion (1)

$$\dot{x} - \Phi(x, u, \pi, \tau) = 0, \quad 0 \le \tau \le 1 \quad (3)$$

and the non-differential constraints

$$S(x, u, \pi, \tau) = 0 \quad , \quad 0 \le \tau \le 1 \quad (4)$$

with the boundary conditions

$$y(0) = \text{given} \quad (5)$$

$$\left[\omega(z, \pi)\right]_0 = 0 \quad (6)$$

$$\left[\psi(x, \pi)\right]_f = 0 \quad (7)$$

where $x(\tau)$ is an n-dimensional state vector, $u(\tau)$ is an m-dimensional control vector and π is a p-dimensional parameter vector. The state $x(\tau)$ is partitioned into vector $y(\tau)$ and $z(\tau)$, defined as follows: $y(\tau)$ is an a-vector that includes the components of $x(\tau)$ whose initial values are given, and $z(\tau)$ is a b-vector that includes the components of $x(\tau)$ that do not belong to $y(\tau)$. Consequently, initial conditions are given as follows:

$$\begin{cases} y(0) = \left[y_l(\tau)\right]_0 \; (l = 1, a) \\ z(0) : \textit{free} \end{cases} \quad (8)$$

$$x(\tau)^T = \left\{ y(\tau)^T, z(\tau)^T \right\} \quad (9)$$

In the above equations, I, f, g, h are scalar, the functional Φ is an n-vector, the function ω is a c-vector, the function ψ is a q-vector, and the function S is a k-vector, $k \le m$.

Derivation of the optimality conditions

From calculus of variation, it can be seen that this problem is one of the Bolza type, and it can be recast as that of minimizing the augmented functional

$$\begin{aligned} J &= (h + \sigma^T \omega)_0 + (g + \mu^T \psi)_1 \\ &\quad + \int_0^1 \left[f + \lambda^T(\dot{x} - \Phi) + \rho^T S \right] dt \\ &= (-\lambda^T x + h + \sigma^T \omega)_0 \\ &\quad + (\lambda^T x + g + \mu^T \psi)_1 \\ &\quad + \int_0^1 \left[f - \lambda^T \Phi + \rho^T S - \dot{\lambda}^T x \right] dt \end{aligned} \quad (10)$$

subject to equations (3)-(7). Here, the n-vector $\lambda(\tau)$ is a time-variable Lagrange multiplier, k-vector $\rho(\tau)$ is a time-variable Lagrange multiplier, c-vector σ is a constant Lagrange multiplier, and the q-vector μ is a constant Lagrange multiplier. The second form of equation (10) arises after the customary integration by parts is performed.

In order to solve the stated problem, the function $x(\tau)$, $u(\tau)$, π and the multipliers $\lambda(\tau)$, $\rho(\tau)$, σ, μ must satisfy the feasibility equations (3)-(7) and the following optimality conditions:

$$\dot{\lambda} - f_x + \lambda^T \Phi_x - \rho^T S_x = 0, \quad 0 \le t \le 1 \quad (11)$$

$$f_u - \lambda^T \Phi_u + \rho^T S_u = 0, \quad 0 \le t \le 1 \quad (12)$$

$$(h_\pi + \sigma^T \omega_\pi)_0 + (g_\pi + \mu^T \psi_\pi)_1 + \int_0^1 \left[f_\pi + \lambda^T \Phi_\pi + \rho^T S_\pi \right] dt = 0 \quad (13)$$

$$(-\zeta + h_z + \sigma^T \omega_z)_0 = 0 \quad (14)$$

$$(\lambda^T + g_x + \mu^T \psi_x)_1 = 0 \quad (15)$$

where $\zeta(\tau)$ is a b-vector and the components of $\lambda(\tau)$ associated with $z(\tau)$.

In this formulation, a time normalization is used in order to simplify the numerical calculation for this problem. That is, the actual time t is replaced by the normalized time $\tau = t / \theta$, which is defined in such a way that the initial time is $\tau = 0$ and the final time is $\tau = 1$. The actual final time θ, if it is free, is regarded as a component of the vector parameter π to be optimized. In this way, the optimal control problem with variable final time is converted into an optimal control problem with fixed final time. With this formulation, several numerical algorithms, SCGRA, MQA, etc., were developed by Miele et al[2),4)]. In this paper, SCGRA and MQA are utilized to calculate numerical optimal trajectories.

III. The application to the formulation of minimum time-to-overtake problems

In this section, it is shown that the general formulation of optimal control problems considered in Sec. II can be applied to the formulation of the minimum time-to-overtake problems. The necessary conditions are partly modified assuming a Meyer problem formulation.

Equations of motion

The equations of motion for the aircraft in the 3-Dimensional space are the following (see Fig. 1 and Fig. 2 for nomenclature)

$$\dot{x} = V\cos\gamma\cos\psi \quad (16)$$

$$\dot{y} = V\cos\gamma\sin\psi \quad (17)$$

$$\dot{z} = V\sin\gamma \quad (18)$$

$$m\dot{V} = T\cos\alpha - D - mg\sin\gamma \quad (19)$$

$$mV\dot{\gamma} = (T\sin\alpha + L)\cos\sigma - mg\cos\gamma \quad (20)$$

$$mV\dot{\psi} = \{(T\sin\alpha + L)\sin\sigma\}/\cos\gamma \quad (21)$$

where $\dot{x}$ denote dx/dt, for example. Aircraft masses are assumed to be constant.

In above equations, aerodynamic forces can be written with their aerodynamic coefficients as follows:

$$L = \frac{1}{2}\rho V^2 A_W C_L, \quad C_L = C_{L\alpha}\,\alpha \quad (22)$$

$$D = \frac{1}{2}\rho V^2 A_W C_D, \quad C_D = C_{D0} + \kappa C_L^2 \quad (23)$$

and atmospheric density can be described in an exponential expression as follows:

$$\rho = \rho_0 \exp(-cz) \quad (24)$$

where it holds the unit in kilogram per cubic meter.

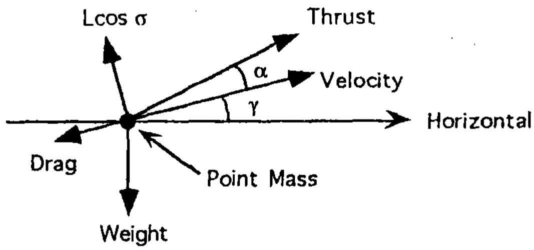

Fig. 1 Forces in the Flight (SIDE VIEW)

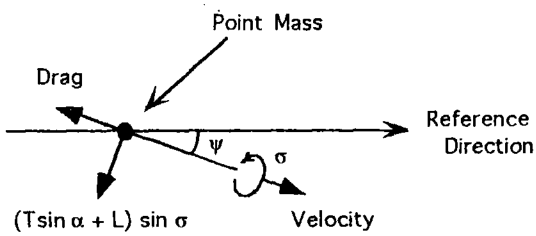

Fig. 2 Forces in the Flight (TOP VIEW)

Constraints

In this problem, control variables are the angle of attack α, the thrust T, and the bank angle σ. These controls are usually constrained between some upper and lower degree of limitation. That is,

$$|C_L| \le C_{L\max}, \quad |\alpha| \le \alpha_{\max} \quad (25)$$

$$0 \le C_T \le C_{T\max} \quad (26)$$

which is provided by the performance and aerodynamic characteristics of aircraft. There is, in addition, an upper and lower limit on the normal acceleration that can be expressed as

$$n_{\min} \le n \le n_{\max} \quad (27)$$

where $n_{\max}$ is the maximum allowable normal acceleration in g (maximum load factor) and $n_{\min}$ is the minimum allowable normal acceleration in g (minimum load factor). These limits are determined by the structural limitation of aircraft and/or the average physiological limitation of the pilot. In fact, $n_{\min}$ is often denoted by negative sign. Besides, load factor n and angle of attack α are connected with equality expression

$$n = \frac{\rho V^2 A_W C_{L\alpha}\,\alpha}{2mg} \quad (28)$$

Now the components for the formulation corresponding to the eqs.(3)-(15) appeared all together except for the performance index and boundary conditions, one thing remains intact. The inequality constraint eqs.(25)-(27) should be converted into equality constraint for the convenience of calculating the general formulation of optimal control problems exactly. Then the introduction of dummy control variables is required for this purpose. With the use of the dummy variables, u_α, u_T, and u_n, eqs.(25)-(27) can be rewritten as follows:

$$\alpha - \alpha_{\max}\sin u_\alpha = 0, \quad \left(-\frac{\pi}{2} \le u_\alpha \le \frac{\pi}{2}\right) \tag{29}$$

$$C_T - \frac{C_{T\max}}{2}\left(1+\sin u_T\right) = 0, \quad \left(-\frac{\pi}{2} \le u_T \le \frac{\pi}{2}\right) \tag{30}$$

$$n - \left\{\frac{n_{\max}-n_{\min}}{2}\left(1+\sin u_n\right) + n_{\min}\right\} = 0, \quad \left(-\frac{\pi}{2} \le u_n \le \frac{\pi}{2}\right) \tag{31}$$

The advantage of the use of dummy control variables is that it need only the eq. (12) for optimality condition of control variables to carry out this formulation into calculations.

IV. Numerical Results of the Minimum Time-To-Overtake Problems

To illustrate the characteristics of optimal control problems with inequality constraints on control variables in the previous two sections, here we consider the problem of finding the low-thrust aircraft trajectories to overtake an opponent aircraft performing some steady-state level turning flight. In the following subscript T denotes the state quantities on the steady-state level turning aircraft (evader) and subscript 0 denote the state quantities on the pursuing aircraft (pursuer).

The performance index is expressed as

$$J = t_f = \int_0^{t_f} \mathrm{d}t \tag{32}$$

The initial and final conditions for evader are all specified except for the final heading, which is given by

$$\begin{aligned} x_{Ti} &= 973.55\ [m] & V_{Ti} &= 0.4\ [Mach] \\ y_{Ti} &= 197.35\ [m] & \gamma_{Ti} &= 0\ [\deg] \\ z_{Ti} &= 5000\ [m] & \psi_{Ti} &= 22.92\ [\deg] \end{aligned} \tag{33}$$

$$R = 2500\ [m],\quad z_0 = 5000\ [m] \tag{34}$$

$$R\psi_{Ti} = 1000\ [m] \tag{35}$$

$$\begin{aligned} x_{Tf} &= R\sin\psi_{Tf} & V_{Tf} &: \text{constant} \\ y_{Tf} &= R(1-\cos\psi_{Tf}) & \gamma_{Tf} &= 0 \\ z_{Tf} &= z_0 & \psi_{Tf} &= \psi_{0f} \end{aligned} \tag{36}$$

And the initial and final conditions of pursuer are given by

$$\begin{aligned} x_{0i} &= 0\ [m] & V_{0i} &= V_0\ [Mach] \\ y_{0i} &= 0\ [m] & \gamma_{0i} &= 0\ [\deg] \\ z_{0i} &= 5000\ [m] & \psi_{0i} &= 0\ [\deg] \end{aligned} \tag{37}$$

$$V_0 = 0.4,\ 0.6,\ 0.8\ [Mach] \tag{38}$$

$$\begin{aligned} x_{0f} &= x_{Tf} & V_{0f} &: free \\ y_{0f} &= y_{Tf} & \gamma_{0f} &= 0 \\ z_{0f} &= z_0 & \psi_{0f} &= \psi_{Tf} \end{aligned} \tag{39}$$

Fig.3 shows the illustration of numerical calculation model by means of Cartesian coordinates.

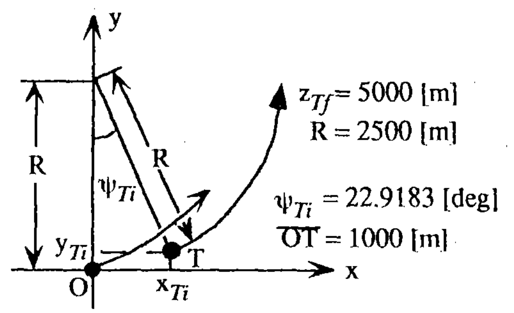

O(x_{0i}, y_{0i}, z_{0i}) = (0, 0, 5000) [m]
T(x_{Ti}, y_{Ti}, z_{Ti}) = ($R\sin\psi_{Ti}$, $R(1-\cos\psi_{Ti})$, 5000) [m]

Fig. 3 Illustration of Numerical Calculation Model (TOP VIEW)

Other necessary constants are as follows:

$$\begin{aligned} C_{D0} &= 0.0665 & c &= 1.018\times10^{-4} \\ C_{L\alpha} &= 4.0 & k &= 0.1412 \\ C_{T\max} &= 0.7 & \rho_0 &= 1.225\ [kg/m^3] \end{aligned} \tag{40}$$

$$A_w = 27.88 \ [m^2] \quad m = 10348 \ [kg]$$
$$n_{max} = 10.0 \quad n_{min} = -4.0 \quad (41)$$
$$g = 9.8 \ [m/s^2] \quad a = 340 \ [m/s]$$

The numerical calculations are made in the following combinations I, II, and III in Table. 1, which shows the initial velocity of evader and pursuer in eq.(33) and (38), that make the conditions easy to compare.

	I	II	III
Vanguard : V_{Ti} [*Mach*]	0.4	0.4	0.4
Pursuer : V_{0i} [*Mach*]	0.4	0.6	0.8

Table. 1: Comparison of the Type of Calculation by the Initial Flight Velocity

The results of unspecified final state variables and time are presented in Table. 2, and the results at overtaking point when pursuer runs the same trajectory after evader are presented in Table. 3.

	I	II	III
V_{0f} [*Mach*]	0.5635	0.6529	0.7844
ψ_f [deg]	84.87	58.96	45.41
t_f [sec]	19.876	11.563	7.2163

Table. 2: Results of Free State Variables and Time

	I	II	III
ψ_f [deg]	N/A	68.75	45.84
t_f [sec]	N/A	14.706	7.3529

Table. 3: Case for Stead-State Turning Pursuer (Pursuer runs the same trajectory after evader with steady-state)

The numerical results of overall optimal trajectories are shown in Fig. 5 through Fig. 11. The resulting optimal flight paths obviously dive in the first half of the flight and then rise up in the latter half in Fig. 6. This is the characteristic flight path of the low speed yo-yo maneuver. Evidently, the lesser the initial velocity of pursuer is, the greater the rate of decent is. Moreover, the latter half of the flight always looks like relatively radical maneuver for pursuer, which can also be understood in Fig. 7 and Fig. 10. Maneuver can be explained by a trade-off between kinetic and potential energy of aircraft. In general, pursuer is going to compensate initial distance to the opponent or time behind toward the evader with the increase of his velocity somehow in the flight. The reason for this rapid motion is that the conversion of potential energy into kinetic energy is quicker than thrust control to change the speed of the aircraft. In order to convert potential energy into kinetic energy, pursuer lowers the angle of attack early in the flight. These consecutive movements might also improve its acceleration performance of aircraft in order to decrease the drag. To increase the velocity to some extent in the first half contributes to retrieving the initial distance or time behind, and furthermore, aircraft does not lose total energy much during the yo-yo maneuver except at the end, when the angle of attack is maximum to make the path angles meet the final boundary condition (see Fig. 11) . The lesser the initial velocity of pursuer is, the more time to put on speed pursuer have. The trajectories have also rather asymmetrical shape. That is because thrust is taken into account to the formulation. From Fig. 8, it can be seen that thrust control takes maximum value all the way in the optimal flight.

V. Conclusions

In this paper, minimum-time 3-Dimensional turns to overtake an opponent aircraft flying in steady-state level turning with constant velocity and initial distance are numerically analyzed. The results of the optimal maneuver form a sequence of low speed yo-yo maneuver trajectories, which can be clearly understood the effectiveness of this maneuver throughout the behavior of some state and control variables. Also, the effectiveness is manifested by the relatively low initial velocity aircraft. When the initial velocity is high, it may result in the high speed yo-yo maneuver.

References

1)Bryson, A.E. and Ho, W.C., *Applied Optimal Control*, Ginn- Blaisdell, Waltham, Mass., 1969.

2)Wu, A.K., et al., *Optimal Control Applications & Methods*, 1-1, pp.69-88, 1980

3)Miele, A., et al., *Journal of Optimization Theory and Applications*, 14-5, 529-556, 1974

4)Gonzalez, S., et al. , *Journal of Optimization Theory & Applications*, 50, pp.109-128, 1986

— - : Evader Flight Path (V_0 = 0.4 [Mach])
This aircraft was caught up with Pursuer-I at 84.87 deg.

—— : Pursuer-I Flight Path (V_0 = 0.4 [Mach])

- - - : Evader Flight Path (V_0 = 0.4 [Mach])
This aircraft was caught up with Pursuer-II at 58.96 deg.

—— : Pursuer-II Flight Path (V_0 = 0.6 [Mach])

- - - : Evader Flight path (V_0 = 0.4 [Mach])
This aircraft was caught up with Pursuer-III at 45.41 deg.

—— : Pursuer-III Flight Path (V_0 = 0.8 [Mach])

Fig. 4 : PLOT LEGEND

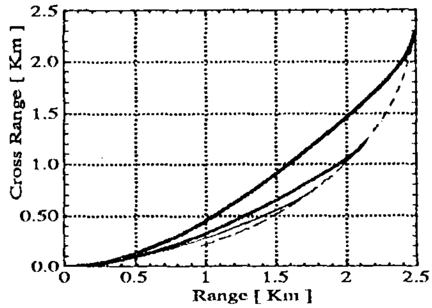

Fig.5 : EVADER-PURSUER FLIGHT PATH

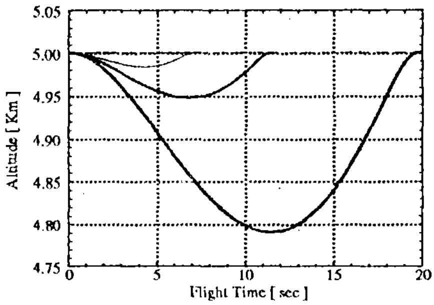

Fig. 6 : TIME HISTORY OF VARING ALTITUDE

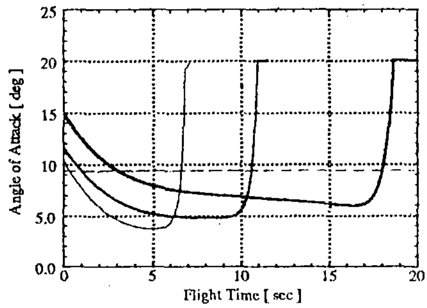

Fig. 7 : TIME HISTORY OF ANGLE OF ATTACK

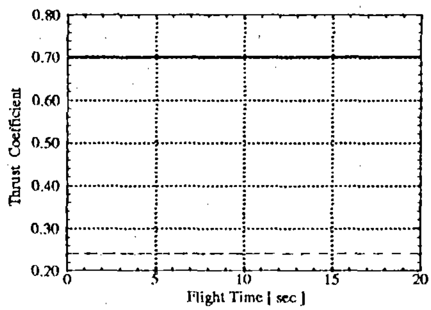

Fig. 8 : TIME HISTORY OF THRUST COEFFICIENT

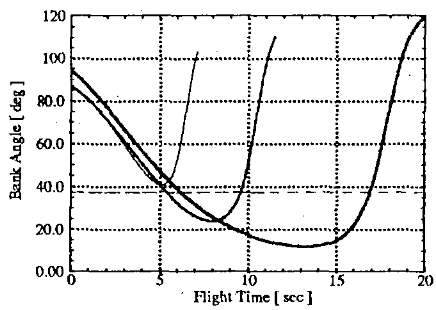

Fig. 9 : TIME HISTORY OF BANK ANGLE

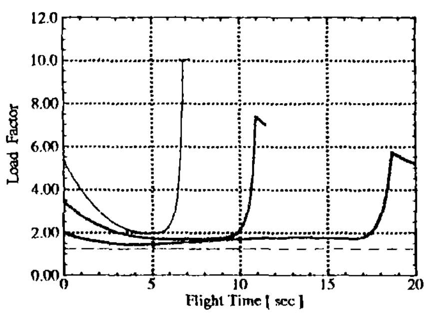

Fig. 10 : TIME HISTORY OF LOAD FACTOR

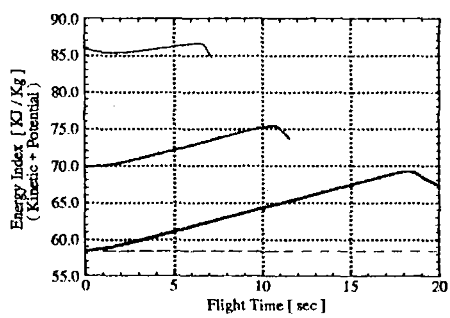

Fig. 11 : TIME HISTORY OF ENERGY TRANSITION